

# Therapeutic Effect of Doxorubicin-Chlorin E6-Loaded Mesoporous Silica Nanoparticles Combined with Ultrasound on Triple-Negative Breast Cancer

This article was published in the following Dove Press journal:  
*International Journal of Nanomedicine*

Peng Xu <sup>1,2,\*</sup>  
Jia Yao <sup>1,\*</sup>  
Zhen Li <sup>3,\*</sup>  
Meng Wang <sup>2</sup>  
Linghui Zhou <sup>1,2</sup>  
Guansheng Zhong <sup>1</sup>  
Yi Zheng <sup>1,2</sup>  
Na Li <sup>1,2</sup>  
Zhen Zhai <sup>1,2</sup>  
Si Yang <sup>1,2</sup>  
Ying Wu <sup>1,2</sup>  
Dai Zhang <sup>2</sup>  
Zhijun Dai <sup>1</sup>

<sup>1</sup>Department of Breast Surgery, The First Affiliated Hospital, College of Medicine, Zhejiang University, Hangzhou 310003, People's Republic of China; <sup>2</sup>Department of Oncology, The Second Affiliated Hospital of Xi'an Jiaotong University, Xi'an 710004, People's Republic of China; <sup>3</sup>Department of Student Affairs, The Second Affiliated Hospital of Xi'an Jiaotong University, Xi'an 710004, People's Republic of China

\*These authors contributed equally to this work

Correspondence: Zhijun Dai  
Department of Breast Surgery, The First Affiliated Hospital, College of Medicine, Zhejiang University, Hangzhou 310003, People's Republic of China  
Tel +86 571 8723 6852  
Email dzj0911@126.com

**Introduction:** Sonodynamic Therapy (SDT) has good targeting and non-invasive advantages in solid cancers, but its antitumor effect is not sufficient to replace traditional treatments. Some studies that combined SDT with chemotherapy or nanoparticles have managed to enhance its efficiency and overcome the side effects of chemotherapy.

**Materials and Methods:** In this study, we synthesized and characterized mesoporous silica nanoparticles (MSN-DOX-Ce6) loaded with doxorubicin (DOX) and sonosensitizer, chlorin e6 (Ce6). Then, we conducted in vitro and in vivo experiments to explore the antitumor effect of MSN-DOX-Ce6 under ultrasound (US) treatment.

**Results:** The characterization tests showed that the nanoparticles are uniformly sized spheres with mesoporous structure, resulting in a high drug-loading efficiency. In the in vitro experiments, MSN-DOX-Ce6 could effectively inhibit cell proliferation under US but not more than other treatment groups. However, the in vivo studies showed that MSN-DOX-Ce6+US has better antitumor effect than DOX+Ce6+US or DOX alone on xenograft tumor-bearing mice.

**Conclusion:** In summary, MSNs showed a great potential for DOX and Ce6 delivery. We concluded that under US, MSN-DOX-Ce6 nanocomposites increase the antitumor effect of DOX and SDT and thereby are a potential treatment for solid tumors.

**Keywords:** sonodynamic therapy, co-delivery, combination chemotherapy, nanomaterials

## Introduction

Triple-negative breast cancer patients at metastatic stage have a poor prognosis due to lack of efficient targeted therapies.<sup>1</sup> The treatment characteristics are severe, so it is urgent to find new agents and therapies.

Sonodynamic therapy (SDT) was first introduced by Umemura in the 1990s to treat cancer.<sup>2,3</sup> SDT uses ultrasound (US) to trigger sound-sensitive agents to exert cytotoxic effects. Therefore, compared with photodynamic therapy (PDT), SDT not only has superior targeting and non-invasive properties, but also is more suitable for deeper tumors.<sup>4,5</sup> The mechanisms of SDT have not yet been clearly explored. The accepted explanations include the generation of sonosensitizer-derived reactive oxygen species (ROS)<sup>6-8</sup> that initiate the oxidation of membrane lipid components and the physical destabilization of the ultrasound-related cell structure that makes the cell more susceptible to the mechanical shear force and cavitation enhancing cell membrane drug transportation (sonoporation). Sonosensitizers such as porphyrins,<sup>9</sup> chlorins,<sup>10</sup> and phthalocyanines,<sup>11</sup> which are typically used as

photosensitizers, have been extensively studied for cancer treatment through SDT.<sup>12</sup> Nowadays, only a few advanced-stage cancer patients receive SDT in addition to chemotherapy, hormonal therapy, and immunotherapy.<sup>13–15</sup> In most of these cases, SDT showed excellent efficacy, resulting in a positive clinical outcome. Although both preclinical and clinical studies confirmed that SDT is effective against malignant tumors, it may not be used alone in treating cancer.

In order to enhance the anticancer activity of SDT, potential enhancements in the SDT activity were explored through new sonosensitizers,<sup>6,7</sup> drug delivery strategies, and combinations with other treatments.<sup>16,17</sup> Some organic and inorganic drug delivery systems have been synthesized aiming at tumor-specific delivery through the enhanced permeability and retention effect (EPR effect)<sup>18,19</sup> and antibody binding.<sup>20</sup> Microbubbles<sup>21</sup> and liposomes<sup>22,23</sup> can deliver high drug doses to the tumor site. However, due to the unstable physicochemical properties of the organic systems, it is difficult to control the outcomes. Alternatively, inorganic materials, such as mesoporous silica nanoparticles (MSNs), titanium dioxide (TiO<sub>2</sub>),<sup>24</sup> manganese dioxide (MnO<sub>2</sub>),<sup>25</sup> and gold nanoparticles<sup>26</sup> display more adaptable and unique properties, such as chemical/thermal stability, tunable pore size, and high surface area.<sup>27</sup> TiO<sub>2</sub> nanoparticles can be activated by US to produce ROS and to exhibit a more significant antitumor effect than either DOX or SDT alone.<sup>24</sup> MnO<sub>2</sub> nanoparticles were not only designed as drug delivery systems but also as hydrogen peroxide decomposition catalysts that improve the tumor's hypoxic environment and as MRI imaging agents.<sup>28</sup> According to previous articles,<sup>29,30</sup> MSNs have good in vivo bio-safety and can reduce the cardiotoxicity of doxorubicin. In addition, the abundant MSN surface silanol groups can react with other functional groups, providing MSNs with a well-modified surface.<sup>19,31,32</sup> Besides a high drug-loading ability, MSNs were also shown to efficiently produce a sonodynamic effect and to significantly inhibit mouse Hep-2 and Lewis carcinoma.<sup>33</sup> In the recent years, many studies involving sonosensitizer-loaded nanomaterials alongside SDT achieved a better antitumor effect.<sup>5</sup>

Therefore, aiming to explore the efficacy of the DOX and SDT combination, we prepared and characterized mesoporous silica nanoparticles loaded with DOX and Ce6 (MSN-Ce6-DOX NPs) and tested the in vitro and in vivo antitumor efficiency on the triple-negative breast cancer cell line (MDA-MB-231).

## Materials and Methods

### Materials

Cetyltrimethylammonium bromide (CTAB), tetraethyl orthosilicate (TEOS), and aminopropyltriethoxysilane (APTES) were purchased from Sigma-Aldrich LLC (Shanghai, China). Doxorubicin hydrochloride (DOX, 98%) and succinic anhydride were supplied by Shanghai Yuanye Bio-Technology Co., Ltd (Shanghai, China). Chlorin e6 (Ce6) was obtained from Frontier Scientific, Inc. (USA). Triethylamine, Glycol, and Toluene were purchased from Tianjin Tianli Chemical Reagent (Tianjin, China). Sodium hydroxide (NaOH, 0.1022 mol/L) was supplied by Tianjin Kemiou Chemical Reagents Co., Ltd (Tianjin, China). Anhydrous ethyl alcohol and ammonium hydroxide were supplied by the Guangdong Chemical Reagent Engineering Technology Research and Development Center (Guangdong, China). Dimethyl sulfoxide (DMSO) was supplied by Tianjin Fuyuhuaogong Co., Ltd (Tianjin, China). All solvents (GR grade) were used without further purification.

The MDA-MB-2231 cells were purchased from Procell Life Science&Technology Co., Ltd (Hubei, China). The BALB/c nude female mice were purchased from Laboratory Animal Center of Medical College of Xi'an Jiaotong University (Shaanxi, China).

### Preparation and Properties of Mesoporous Silica Nanoparticles

#### Preparation of Mesoporous Silica Nanoparticles

MSNs were synthesized according to the published literature.<sup>31,34–36</sup> Initially, 3 mL absolute ethanol and 13 mL deionized water were mixed. Then, 352 mg CTAB and 2 mL sodium hydroxide solution (0.1022 mol/L) were added into and dissolved by stirring at 1000 rpm. Next, a mixture of 2 mL absolute ethanol and 500  $\mu$ L TEOS was added dropwise to the above reaction system. Subsequently, the reaction system was sealed and stirred for 24 h. Later, the milky-white solution was centrifuged at 10,000 rpm for 10 min, and the white precipitate was washed three times with absolute ethanol and deionized water, then dried in a 50°C electric blast drying oven and was labeled MSN-CTAB. Finally, the MSN-CTAB was calcined at 550°C for 6 h to remove the CTAB and to obtain MSNs, labeled MSN-OH.

#### Amination of Mesoporous Silica Nanoparticles

Five hundred milligrams of MSN-OH was ultrasonically dispersed in 25 mL toluene. Afterwards, 100  $\mu$ L APTES

was added and the mixture was continuously stirred for 4 h at 50°C. The precipitate was collected by centrifuging for 10 min at 10,000 rpm, washed three times with toluene solution, dried overnight at 120°C, and labeled MSN-NH<sub>2</sub>.

### Carboxylation of Mesoporous Silica Nanoparticles

First, 200 mg MSN-NH<sub>2</sub>, 85 mg succinic anhydride, 10 mL DMSO, and 85 mL triethylamine were mixed and continuously stirred for 48 h at 50°C. Next, the precipitate was collected and washed with absolute ethanol and deionized water, dried overnight at 50°C, and labeled MSN-COOH.

### Drug-Loading Test of Mesoporous Silica Nanoparticles

First, 10 mg MSN-COOH was dispersed in 2 mL PBS (PH 7.40). Afterwards, 1 mL DOX solution (4 mg/mL) and 1 mL Ce6 solution (8 mg/mL) were added to the above mixture and stirred in the dark for 48 h at 1000 rpm. Then, the products were collected by centrifugation (10,000 rpm, 10 min) and gently washed with PBS three times to remove unloaded drugs before drying. The concentrations of DOX and Ce6 in the supernatant were determined with a fluorescence spectrophotometer. The drug loading and encapsulation efficiencies were further calculated by the following formulas:

$$\text{Loading capacity (wt\%)} = \frac{\text{mass of total drug} - \text{mass of drug in supernatant}}{\text{mass of total MSN} - \text{DOX} - \text{Ce6}} \times 100\%$$

$$\text{Encapsulation capacity (wt\%)} = \frac{\text{mass of total drug} - \text{mass of drug in supernatant}}{\text{mass of total drug}} \times 100\%$$

### Mesoporous Silica Nanoparticles Release Test

MSN-DOX-Ce6 (8 mg) were soaked in 4 mL PBS (PH=7.4) and then transferred into a dialysis tube with a molecular weight cutoff (MWCO) of 3500 Da. The sealed dialysis tube was immersed in 18 mL of PBS solution and gently shaken for 24 h at 37°C. Samples of 2 mL dialysate were taken out at 0, 0.25, 0.5, 1, 2, 4, 6, 8, 10, 12, 18, and 24 h for ultraviolet fluorescence analysis. Subsequently, the dialysate was replenished with an equal volume of PBS.

### Characterization and Detection of Mesoporous Silica Nanoparticles

The morphology and size of the nanoparticles were observed via transmission electron microscopy (TEM, HITACHI, HT7700, Japan). Nitrogen adsorption and desorption capacity as well as the surface area and pore diameter were measured by an Automatic Physical Adsorption Meter (model ASAP

2020 Plus HD88). MSN-CTAB and MSN-OH were degassed for 8 h at 250 °C before testing and measured under a nitrogen atmosphere at -196°C. The particle size and the potential distribution of the nanoparticles, including MSN-OH, MSN-NH<sub>2</sub> and MSN-COOH, were detected via ZETA potential and nanoparticle size analyzer (Malvern, UK) under deionized water conditions. The measurement parameters were particle size, laser wavelength - 633 nm, measurement angle - 173°, temperature - 28°C, power - 4 MW. Drug load and release efficiencies were determined using a fluorescence spectrophotometer (Hitachi, JAPAN).

### In vitro Antitumor Effect of MSN-DOX-Ce6 Combined with US Cell Uptake Experiment in vitro

The MDA-MB-231 cells were diluted into 2×10<sup>6</sup>/mL with serum-containing medium, transferred into 6-well plates, and cultured in a 5% CO<sub>2</sub> incubator for 24 h at 37°C. Subsequently, these cells were separately incubated in the normal medium (control group), Dox medium solution, Ce6 medium solution, and MSN-DOX-Ce6 medium solution. The concentrations for each group were Ce6 - 3 µg/mL, DOX - 1 µg/mL, and MSN-DOX-Ce6 (with a considerable dose of DOX). The cells were continually cultured for 30 min, 1 h, 2 h, and 4 h; the medium was then removed and the DOX, Ce6, and MSN-DOX-Ce6 uptake was determined by fluorescence microscopy. It should be noted that the whole process was protected from light. To avoid the precipitation and aggregation of drug-loaded nanoparticle solutions, it was prepared right before it was ready in vitro and vivo experiment.

### Cell Proliferation Inhibition Test

MDA-MB-231 cells were harvested at the logarithmic growth phase and diluted to 2×10<sup>5</sup>/mL with complete medium. Next, 30 clear tubes were prepared and separated into 5 groups. Afterwards, a 1 mL cell suspension and a 1 mL drug solution (containing increasing drug concentrations) were added into each tube: Group A (MSN-DOX-Ce6+US): 0, Ce6 3/DOX 1, Ce6 6/DOX 2, Ce6 12/DOX 4, Ce6 24/DOX 8, Ce6 48/DOX 16 (µg/mL). Group B (DOX+Ce6+US): 0, Ce6 3/DOX 1, Ce6 6/DOX 2, Ce6 12/DOX 4, Ce6 24/DOX 8, Ce6 48/DOX 16 (µg/mL). Group C (Ce6+US): 0, Ce6 3, Ce6 6, Ce6 12, Ce6 24, Ce6 48 (µg/mL). Group D (DOX): 0, DOX 1, DOX 2, DOX 4, DOX 8, DOX 16 (µg/mL). Group E (MSN): a concentration of MSN consistent with Group A.

The cell suspension was mixed and cultured for 4 h in the cell culture incubator. Next, groups A, B, and C were treated

with ultrasound ( $0.5 \text{ W/cm}^2$ ) for 1 min in a medium of degassed water, with a thickness of 1 cm. Afterwards, the suspension from all tubes was added to 96-well plates at 100  $\mu\text{L}$  per well with 6 parallel replicates for each dose group. Subsequently, 96-well plates were cultured for 24 h. Later, 20  $\mu\text{L}$  of CCK-8 solution was added into each well and mixed gently. The cells were cultured for two additional hours, and then the optical density (OD) value was measured by a microplate reader at 450 nm. The growth inhibition rate of each group was calculated. The whole process was protected from light.

### Antitumor Effect of MSN-DOX-Ce6 Combined with US in vivo

Four-week-old BALB/c nude female mice were subcutaneously implanted with MDA-MB-231 ( $5 \times 10^7/\text{mL}$ , 0.2 mL). When tumors reached an average diameter of 6–8 mm, 24 mice with regular tumor shape (spherical, ellipsoidal) and no ulcer were randomly distributed into 4 groups: control group, DOX, DOX+Ce6+US, and MSN-DOX-Ce6+US. The drugs were administered intravenously every 2 days and five times totally. The drug doses were as follows: DOX, 3 mg/kg; Ce6, 10 mg/kg, and a considerable dose of MSN-DOX-Ce6. The control group was given a corresponding volume of physiological saline solution.

After 4 h following the intravenous injection, a degassed water capsule about 1-cm thick was placed between the ultrasound probe and the tumor. The mice in the Ce6+US and the MSN-DOX-Ce6+US groups were treated by ultrasound at  $4 \text{ W/cm}^2$  for 3 min. During the experiment, the tumors and the bodyweights were measured with an electronic Vernier caliper and an electronic balance every 2 days, and the tumor volumes were calculated with the following formula:  $\text{volume (mm}^3) = \text{length} \times (\text{width})^2/2$ . The mouse tumor samples were collected 9 days after the treatment.

### Data Analysis

The experimental data were statistically analyzed with the SPSS 25.0 software or GraphPad.Prism.7.0.  $P < 0.05$  was considered to indicate a significant difference, and the result was expressed as mean  $\pm$  SD.

## Results

### Preparation and Characteristics of Mesoporous Silica Nanoparticles

TEM was adopted to observe the morphology and particle size of the nanoparticles. As shown in Figure 1A and B, the nanoparticles have circular and mesoporous structures

with uniform size, of which, the black structure is the  $\text{SiO}_2$  skeleton and the light gray area between the skeletons is a mesoporous channel. The particle size of the nanoparticles under the TEM was found to be  $149.5 \pm 12.2 \text{ nm}$  (Mean  $\pm$  SD), which was measured by the ImageJ 1.4 software.

The particle size distribution was detected by the Malvern ZETA Potential and Nanoparticle Size Analyzer (ZSE). As shown in Figure 1C, the size of the MSNs ranged from 122 to 300 nm, most of them being distributed between 160 and 220 nm, which is slightly larger than the TEM result. In some way, this difference may be explained by the dispersion degree and the agglomeration of the nanoparticles under the solution condition. Meanwhile, the potential is shown in Figure 1D. First, the surface is covered by hydroxyl groups (-OH) under aqueous conditions because of the  $\text{SiO}_2$  molecule. Therefore, the potential of MSN-OH is negative at a range of  $-31$  to  $-20 \text{ mV}$ . Subsequently, after the amination reaction, the surface charge is positive and the distribution range is 17 to 37 mV, indicating that the -OH group has been converted to  $-\text{NH}_2$ . Finally, after the carboxylation reaction, the potential is negative and the range is  $-37$  to  $-43 \text{ mV}$ , indicating that the  $-\text{NH}_2$  group has been converted to  $-\text{COOH}$ . It is reported that the absolute value of the zeta potential is related to the stability of the colloidal dispersion, and the system has a good stability if the charge ranges between  $\pm 40$  and  $\pm 60 \text{ mV}$ . Therefore, the nanoparticles finally prepared in this experiment have better stability.

The surface area and the pore diameter of the nanoparticles were detected by a fully automatic physical adsorption instrument. The adsorption-desorption isotherm is shown in Figure 1E and F. According to the definition of International Union of Pure and Applied Chemistry (IUPAC), the gas adsorption isotherm shown in Figure 1F conformed to the adsorption characteristics of mesoporous materials, indicated that the materials prepared in this study are mesoporous materials. The BET surface area before and after calcination was  $76.7572 \text{ m}^2/\text{g}$  and  $866.5512 \text{ m}^2/\text{g}$ , respectively; this indicates that the CTAB template was removed after the calcination, bypassing the mesoporous structure.

### Drug Loading and Releasing Properties of Mesoporous Silica Nanoparticles

First, the concentration-fluorescence intensity standard curve of DOX and Ce6, shown in Figure 2A and B, was derived according to the user guidelines. The drug-loading test results showed that the drug-loading efficiencies were: DOX – 10.53

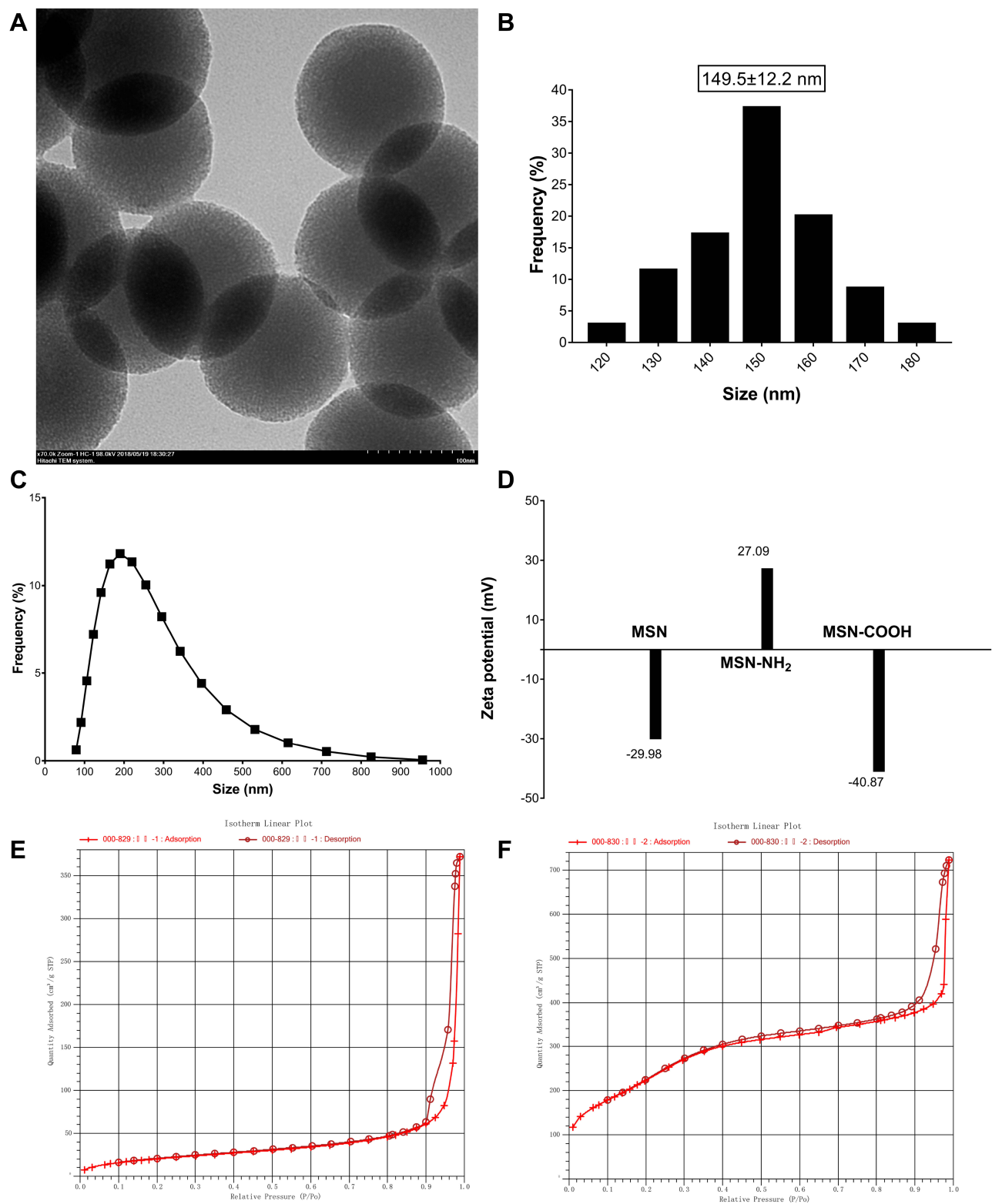


**Figure 1** TEM image (A) and particle sizes (B) of mesoporous silica nanoparticles ( $\times 70.0k$ ). The size distribution curve (C) of MSN and Zeta potential (D) of MSN, MSN-NH<sub>2</sub> and MSN-COOH. N<sub>2</sub> adsorption-desorption isotherms of MSN-CTAB (E) and MSN (F).

**Notes:** The X axis labeling of (E) and (F) is "Quantity Absorbed (cm<sup>3</sup>/g STP)"; the Y axis labeling of (E) and (F) is "relative pressure (P/P<sub>0</sub>)".

**Abbreviations:** TEM, transmission electron microscopy; MSN, mesoporous silica nanoparticle; CTAB, cetyltrimethylammonium bromide.

wt % and Ce6 – 36.84 wt %; the encapsulation efficiencies were: DOX – 50 wt % and Ce6 – 99.5 wt %. Compared to the loading rate of DOX containing MSN prepared by other laboratories, the drug-loaded nanoparticles prepared in this study are co-loaded with DOX and Ce6, with a satisfactory total drug-loading rate and drug-loading performance.

To decrease the influence of liquid volatilization, the experiment was carried out at 25°C. As shown in Figure 2C, the DOX release rate from prepared nanoparticles is lower than that of free DOX due to the obstruction of the physical pores, but 10 h later, the drug release rate reached 80% and increased slowly thereafter. The results of this experiment suggest that MSN-DOX-Ce6 can slow drug release, but does

not exhibit sustained release, which is due to the lack of mesoporous closing on the surface.

### Cell Uptake Test

As shown in Figure 3, there was no fluorescence signal in the control group (normal medium), during the entire test. With increase in duration, weak fluorescence signals in the DOX, Ce6, and MSN-DOX-Ce6 groups were detected at 1 h and 2 h, and stronger signals at 4 h. However, the fluorescence of the MSN-DOX-Ce6 group was not stronger than that of the other two groups, indicating that the nanoparticles may not have the ability to promote cell uptake. We speculate that this is because the cells cultured in vitro lack tissue

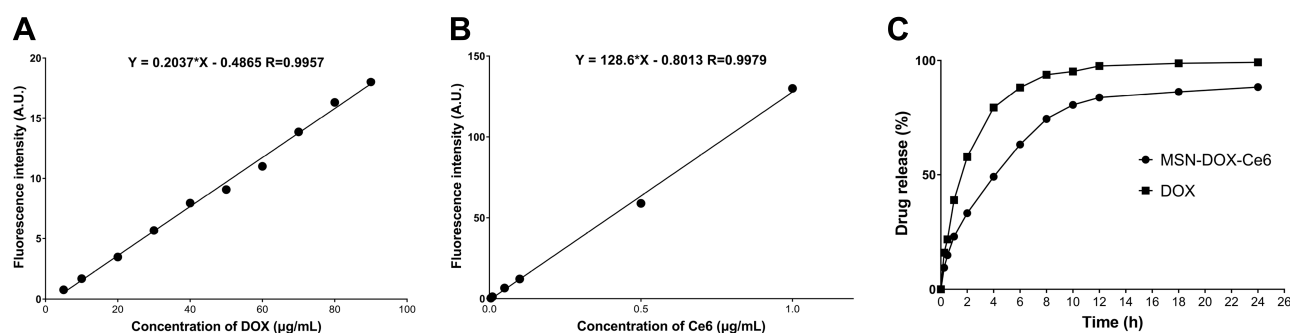


**Figure 2** The concentration-fluorescence intensity standard curve of DOX (A) ( $\lambda_{ex}/em$ : 476/603 nm) and Ce6 (B) ( $\lambda_{ex}/em$ : 408/666 nm). DOX release of MSN-DOX-Ce6 (C). **Abbreviations:** DOX, Doxorubicin hydrochloride; Ce6, Chlorin e6; MSN, mesoporous silica nanoparticle.

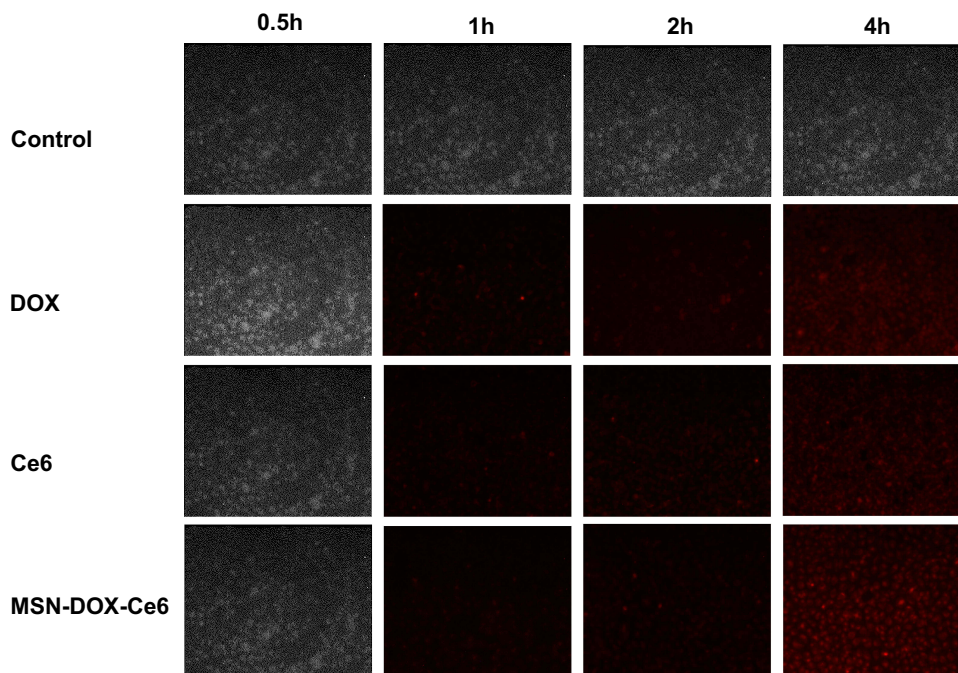


**Figure 3** The confocal laser scanning microscope images of MDA-MB-231 cell lines after co-cultivation with different drugs. **Abbreviations:** MSN, mesoporous silica nanoparticle; DOX, Doxorubicin hydrochloride; Ce6, Chlorin e6.

structure and vasculature and the nanoparticles do not have an EPR effect and cannot exert passive targeting ability. Therefore, drugs released from the nanoparticles and the free drugs both permeate the cells, probably by free diffusion. From another perspective, the results showed that the drugs and the cells need to be co-cultured for 4 h and then sonicated to exert the antitumor effect of Ce6.

## In vitro and in vivo Antitumor Effect

According to the results of the CCK-8 test (Figure 4), as the concentration of MSN increased from 0 to 152  $\mu\text{g/mL}$ , the viability of MDA-MB-231 cells did not significantly decrease, indicating that MSN are safe in this concentration range. On the contrary, the viability of the MDA-MB-231 cells in the other four treatment groups was significantly lower than that of the MSN group ( $P < 0.05$ ). In addition, the cell viability in the MSN-DOX-Ce6+US group was lower than that of Ce6+US, DOX+Ce6+US or DOX ( $P < 0.05$ ). The results also showed that the cell viability between DOX and DOX+Ce6+US groups was not significant. The possible reasons may be that the anticancer effect of SDT is relatively weak compared to that of DOX, which is a widely used antineoplastic agent. When they are combined, the role of doxorubicin is dominant and Ce6+US contributes less to the overall efficacy and does not significantly improve the antitumor effect. Another reason may be related to the mechanism of action of SDT. During sonication, the in vitro cell density is lower than that of the solid tumor and the

ultrasound cavitation effect and the action of singlet oxygen may be affected.

Therefore, we conducted an in vivo experiment to determine the antitumor efficacy of MSN-DOX-Ce6 combined with US. As shown in Figure 5A, after the subcutaneous tumor was formatted, the weight of the mice in the control group did not increase, while the weight of MSN-DOX-Ce6+US group increased, followed by DOX+Ce6+US and DOX groups. According to the weight curve, we found that the drug-loaded nanoparticles combined with ultrasound have a better antitumor effect than DOX+Ce6+US and DOX groups. Next, as shown in Figure 5B, the tumor volume of the MSN-DOX-Ce6+US group did not significantly increase, and the tumor volume of DOX+Ce6+US group and the DOX group showed a certain increase, indicating that MSN-DOX-Ce6+US performed better than other treatments. The metabolism of tumor-bearing mice was significantly affected by decreased synthesis and increased consumption. After the treatment, tumor growth was inhibited, resulting in improved health and increased weight.

Finally, the tumors were harvested and their weight and volume were measured (Figure 6A–C). The weight and volume of the tumors in the control group were higher than those of the other experimental groups ( $P < 0.05$ ), with statistical differences between the MSN-DOX-Ce6+US, DOX, and Ce6+US groups ( $P < 0.05$ ). The results of the in vivo experiment indicated that MSN-DOX-Ce6 combined with ultrasound has a superior therapeutic effect, compared to other therapies. The in vivo study also found that the same dose of DOX, combined with Ce6+US performed better than DOX alone, indicating that SDT has a synergistic effect with chemotherapy.

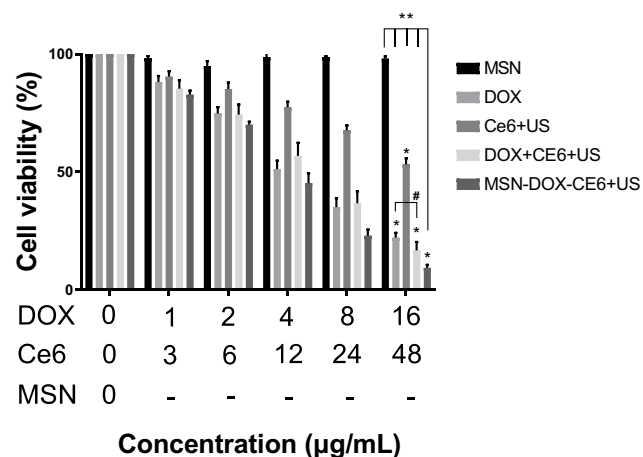


**Figure 4** Cell viability of MDA-MB-231 after different treatments with increased concentration.

**Notes:** “-” means the concentration of MSN consistent with MSN-DOX-Ce6+US Group; \*Means other groups VS MSN  $P < 0.05$ ; \*\*Means MSN-DOX-Ce6+US group vs others  $P < 0.05$ ; #Means  $P > 0.05$ .

**Abbreviations:** MSN, mesoporous silica nanoparticle; DOX, Doxorubicin hydrochloride; Ce6, Chlorin e6; US, ultrasound.

## Discussion

SDT has been developed for many years due to its unique features in the clinical context: satisfactory antitumor efficacy, targeting ability, safety, and noninvasiveness. However, the effect of this therapy is not sufficient to replace traditional antitumor therapies, as it has not yet been widely used clinically. The objective of this article was to explore the possible combination of chemotherapy and SDT through a drug delivery system. In this study, MSN-DOX-Ce6 were successfully prepared by a soft template method. The drug loading and release tests confirmed that the nanoparticles have appropriate morphology, size, and high drug-loading properties, with a shortcoming that we did not modify target proteins or molecules on the

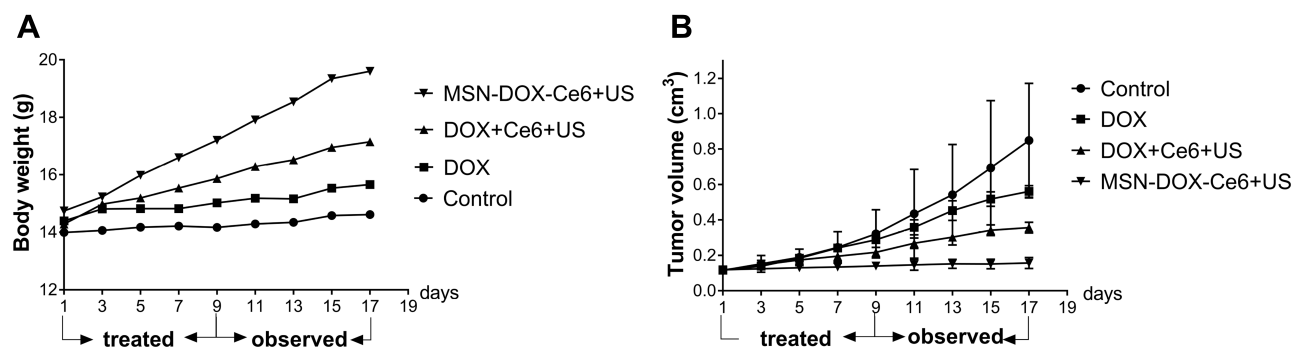


**Figure 5** Body weight (A) and tumor volume (B) of MDA-MB-231 tumor xenografts after different treatments. **Abbreviations:** MSN, mesoporous silica nanoparticle; DOX, Doxorubicin hydrochloride; Ce6, Chlorin e6; US, ultrasound.

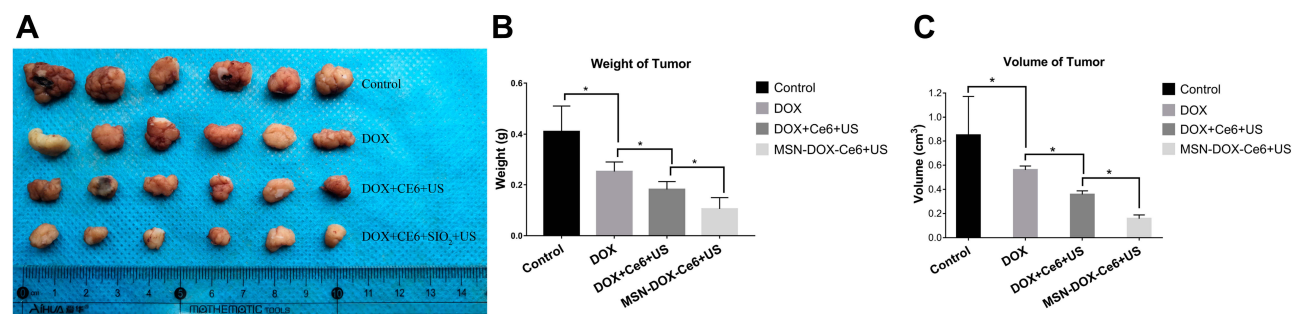


**Figure 6** Images of the tumors (A), tumor’s weight (B) and volume (C) at the end of experiment. (\**p*<0.05). **Abbreviations:** MSN, mesoporous silica nanoparticle; DOX, Doxorubicin hydrochloride; Ce6, Chlorin e6; US, ultrasound.

surface to enhance the targeting ability. The in vitro and in vivo experiments showed that the drug delivery system combined with ultrasound has a better antitumor capacity than DOX or SDT alone. Therefore, we reasoned that after the drug-loaded mesoporous silica nanoparticles entered the blood circulation, MSN-DOX-Ce6 passively targeted and enriched at tumor tissue due to the EPR effect, then released DOX and Ce6 and improved drug concentration around the tumor cells. Following activation by sonication, Ce6 exerted antitumor effects alongside DOX; hence, the antitumor effect of MSN-DOX-Ce6 was stronger than that in the other groups. However, this hypothesis needs to be verified by further studies. What is more, MSN-DOX-Ce6 nanoparticles are not stable over time in solutions, rising major concern for translational applications. This point should be discussed and maybe overcome by surface modification. Nonetheless, our results suggest that the combination of chemotherapy and SDT is a safe and effective method with great potential for cancer treatment. We expect SDT to be extensively used clinically, owing to its enhanced therapeutic effect and reduced side effects.

## Conclusion

In summary, we developed MSN-DOX-Ce6 nanocomposites that can be triggered by ultrasound for an increased antitumor effect, by combining chemotherapy and SDT. Our results suggest that MSN-DOX-Ce6 have superior targeted delivery and controllable activation potential for safe and effective treatment of solid tumors.

## Ethics Approval

The protocol of animal experiments was approved by the Ethics Committee of Xi’an Jiaotong University, and all experimental procedures followed the Provisions and General Recommendation of Chinese Experimental Animals Administration Legislation.

## Acknowledgments

The authors gratefully acknowledge the financial support of the National Natural Science Foundation of China (81471670) and Key R & D projects in Shaanxi Province (2015KTCL03-06). They thank Miss Wang Yu, Mr Chang Gang at core facilities sharing platform of Xi’an Jiaotong University, and



Miss Chen Mingxia at Biomedical Experimental Center of Xi'an Jiaotong University for their assistance with ZETA potential & nanoparticle size analyzer, automatic physical adsorption meter, and transmission electron microscopy analysis.

## Disclosure

The authors report no conflicts of interest in this work.

## References

- Curigliano G, Goldhirsch A. The triple-negative subtype: new ideas for the poorest prognosis breast cancer. *J Natl Cancer Inst Monographs*. 2011;2011(43):108–110. doi:10.1093/jncimonographs/lgr038
- Yumita N, Kawabata K, Sasaki K, Umemura S. Sonodynamic effect of erythrosin B on sarcoma 180 cells in vitro. *Ultrason Sonochem*. 2002;9(5):259–265. doi:10.1016/S1350-4177(02)00080-9
- Umemura S, Yumita N, Nishigaki R, Umemura K. Mechanism of cell damage by ultrasound in combination with hematoporphyrin. *Jpn J Cancer Res*. 1990;81(9):962–966. doi:10.1111/j.1349-7006.1990.tb02674.x
- Liu X-H, Li S, Wang M, Dai Z-J. Current status and future perspectives of sonodynamic therapy and sonosensitizers. *Asian Pac J Cancer Prev*. 2015;16(11):4489–4492. doi:10.7314/APJCP.2015.16.11.4489
- Lafond M, Yoshizawa S, Umemura SI. Sonodynamic therapy: advances and challenges in clinical translation. *J Ultrasound Med*. 2019;38(3):567–580. doi:10.1002/jum.14733
- He Y, Xia X, Xu C, et al. 5-Aminolevulinic acid enhances ultrasound-induced mitochondrial damage in K562 cells. *Ultrasonics*. 2010;50(8):777–781. doi:10.1016/j.ultras.2010.03.004
- Song W, Cui HD, Zhang R, Zheng JH, Cao WW. Apoptosis of SAS cells induced by sonodynamic therapy using 5-aminolevulinic acid sonosensitizer. *Anticancer Res*. 2011;31(1):39–45.
- Shimamura Y, Tamatani D, Kuniyasu S, et al. 5-Aminolevulinic acid enhances ultrasound-mediated antitumor activity via mitochondrial oxidative damage in breast cancer. *Anticancer Res*. 2016;36(7):3607–3612.
- Wang P, Wang X, Zhang K, Gao K, Song M, Liu Q. The spectroscopy analyses of PpIX by ultrasound irradiation and its sonotoxicity in vitro. *Ultrasonics*. 2013;53(5):935–942. doi:10.1016/j.ultras.2012.10.019
- Wang P, Li C, Wang X, et al. Anti-metastatic and pro-apoptotic effects elicited by combination photodynamic therapy with sonodynamic therapy on breast cancer both in vitro and in vivo. *Ultrason Sonochem*. 2015;23:116–127. doi:10.1016/j.ulsonch.2014.10.027
- Abrahamse H, Hamblin MR. New photosensitizers for photodynamic therapy. *Biochem J*. 2016;473(4):347–364. doi:10.1042/BJ20150942
- Pan X, Wang H, Wang S, et al. Sonodynamic therapy (SDT): a novel strategy for cancer nanotheranostics. *Sci China Life Sci*. 2018;61(4):415–426. doi:10.1007/s11427-017-9262-x
- Wang X, Zhang W, Xu Z, Luo Y, Mitchell D, Moss RW. Sonodynamic and photodynamic therapy in advanced breast carcinoma: a report of 3 cases. *Integr Cancer Ther*. 2009;8(3):283–287. doi:10.1177/1534735409343693
- Kenyon JN, Fuller RJ, Lewis TJ. Activated cancer therapy using light and ultrasound - a case series of sonodynamic photodynamic therapy in 115 patients over a 4 year period. *Curr Drug Ther*. 2009;4(3):179–193. doi:10.2174/157488509789055036
- Inui T, Makita K, Miura H, et al. Case report: a breast cancer patient treated with GcMAF, sonodynamic therapy and hormone therapy. *Anticancer Res*. 2014;34(8):4589–4593.
- Osaki T, Ono M, Uto Y, et al. Sonodynamic therapy using 5-aminolevulinic acid enhances the efficacy of bleomycin. *Ultrasonics*. 2016;67:76–84. doi:10.1016/j.ultras.2016.01.003
- Osaki T, Uto Y, Ishizuka M, et al. Artesunate enhances the cytotoxicity of 5-aminolevulinic acid-based sonodynamic therapy against mouse mammary tumor cells in vitro. *Molecules*. 2017;22(4):533. doi:10.3390/molecules22040533
- Maeda H, Nakamura H, Fang J. The EPR effect for macromolecular drug delivery to solid tumors: improvement of tumor uptake, lowering of systemic toxicity, and distinct tumor imaging in vivo. *Adv Drug Deliv Rev*. 2013;65(1):71–79. doi:10.1016/j.addr.2012.10.002
- Wang Y, Zhao Q, Han N, et al. Mesoporous silica nanoparticles in drug delivery and biomedical applications. *Nanomedicine*. 2015;11(2):313–327. doi:10.1016/j.nano.2014.09.014
- Niu F, Yan J, Ma B, et al. Lanthanide-doped nanoparticles conjugated with an anti-CD33 antibody and a p53-activating peptide for acute myeloid leukemia therapy. *Biomaterials*. 2018;167:132–142. doi:10.1016/j.biomaterials.2018.03.025
- Nesbitt H, Sheng Y, Kamila S, et al. Gemcitabine loaded microbubbles for targeted chemo-sonodynamic therapy of pancreatic cancer. *J Control Release*. 2018;279:8–16. doi:10.1016/j.jconrel.2018.04.018
- Dai ZJ, Li S, Gao J, et al. Sonodynamic therapy (SDT): a novel treatment of cancer based on sonosensitizer liposome as a new drug carrier. *Med Hypotheses*. 2013;80(3):300–302. doi:10.1016/j.mehy.2012.12.009
- Moosavian SA, Bianconi V, Pirro M, Sahebkar A. Challenges and pitfalls in the development of liposomal delivery systems for cancer therapy. *Semin Cancer Biol*. 2019. doi:10.1016/j.semcancer.2019.09.025
- Harada Y, Ogawa K, Irie Y, et al. Ultrasound activation of TiO<sub>2</sub> in melanoma tumors. *J Control Release*. 2011;149(2):190–195. doi:10.1016/j.jconrel.2010.10.012
- Abulizi A, Yang GH, Okitsu K, Zhu -J-J. Synthesis of MnO<sub>2</sub> nanoparticles from sonochemical reduction of MnO<sub>4</sub><sup>-</sup> in water under different pH conditions. *Ultrason Sonochem*. 2014;21(5):1629–1634. doi:10.1016/j.ulsonch.2014.03.030
- Li H, Li Z, Liu L, Lu T, Wang Y. An efficient gold nanocarrier for combined chemo-photodynamic therapy on tumour cells. *RSC Adv*. 2015;5(44):34831–34838. doi:10.1039/C4RA17249C
- Bombelli FB, Webster CA, Moncrieff M, Sherwood V. The scope of nanoparticle therapies for future metastatic melanoma treatment. *Lancet Oncol*. 2014;15(1):e22–e32. doi:10.1016/S1470-2045(13)70333-4
- Yang G, Xu L, Chao Y, et al. Hollow MnO<sub>2</sub> as a tumor-microenvironment-responsive biodegradable nano-platform for combination therapy favoring antitumor immune responses. *Nat Commun*. 2017;8(1):902. doi:10.1038/s41467-017-01050-0
- Chen Y, Chen H, Shi J. In vivo bio-safety evaluations and diagnostic/therapeutic applications of chemically designed mesoporous silica nanoparticles. *Adv Mater*. 2013;25(23):3144–3176. doi:10.1002/adma.201205292
- Yu T, Greish K, McGill LD, Ray A, Ghandehari H. Influence of geometry, porosity, and surface characteristics of silica nanoparticles on acute toxicity: their vasculature effect and tolerance threshold. *ACS Nano*. 2012;6(3):2289–2301. doi:10.1021/nn2043803
- Li Z, Li H, Liu L, You X, Zhang C, Wang Y. A pH-sensitive nanocarrier for co-delivery of doxorubicin and camptothecin to enhance chemotherapeutic efficacy and overcome multidrug resistance in vitro. *RSC Adv*. 2015;5(94):77097–77105. doi:10.1039/C5RA15728E
- Liu X, Deng G, Wang Y, et al. A novel and facile synthesis of porous SiO<sub>2</sub>-coated ultrasmall Se particles as a drug delivery nanopatform for efficient synergistic treatment of cancer cells. *Nanoscale*. 2016;8(16):8536–8541. doi:10.1039/C6NR02298G
- Osminkina LA, Kudryavtsev AA, Zinoviyev SV, et al. Silicon nanoparticles as amplifiers of the ultrasonic effect in sonodynamic therapy. *Bull Exp Biol Med*. 2016;161(2):296–299. doi:10.1007/s10517-016-3399-x

34. Fang X, Chen C, Liu Z, Liu P, Zheng N. A cationic surfactant assisted selective etching strategy to hollow mesoporous silica spheres. *Nanoscale*. 2011;3(4):1632–1639. doi:10.1039/c0nr00893a
35. Kresge CT, Leonowicz ME, Roth WJ, Vartuli JC, Beck JS. Ordered mesoporous molecular sieves synthesized by a liquid-crystal template mechanism. *Nature*. 1992;359(6397):710–712. doi:10.1038/359710a0
36. Guo H, Qian H, Sun S, et al. Hollow mesoporous silica nanoparticles for intracellular delivery of fluorescent dye. *Chem Cent J*. 2011;5(1):1. doi:10.1186/1752-153X-5-1

### International Journal of Nanomedicine

Dovepress

### Publish your work in this journal

The International Journal of Nanomedicine is an international, peer-reviewed journal focusing on the application of nanotechnology in diagnostics, therapeutics, and drug delivery systems throughout the biomedical field. This journal is indexed on PubMed Central, MedLine, CAS, SciSearch®, Current Contents®/Clinical Medicine,

Journal Citation Reports/Science Edition, EMBase, Scopus and the Elsevier Bibliographic databases. The manuscript management system is completely online and includes a very quick and fair peer-review system, which is all easy to use. Visit <http://www.dovepress.com/testimonials.php> to read real quotes from published authors.

Submit your manuscript here: <https://www.dovepress.com/international-journal-of-nanomedicine-journal>